Pharmaceutical Research, Vol. 22, No. 6, June 2005 (© 2005)
DOI: 10.1007/s11095-005-4584-1

Research Paper

Pharmacokinetics and Modeling of Quercetin and Metabolites

Xiao Chen,[1,2] Ophelia Q. P. Yin,[1] Zhong Zuo,[1] and Moses S. S. Chow[1,3]

Received September 27, 2004; accepted February 28, 2005

Purpose. To determine the pharmacokinetics of quercetin and its glucuronide/sulfate conjugates and to develop a pharmacokinetic model to simultaneously describe their disposition after intravenous and oral administration in rats.
Methods. After oral, intraportal, and intravenous administration of quercetin, serial plasma, urine, and fecal concentrations of quercetin and its conjugates were determined by an HPLC method. Enterohepatic recirculation was evaluated in a linked-rat model as well as after oral administration of bile containing quercetin and its metabolites. Based on the experimental data, a specific compartmental model was developed and validated to describe and predict the plasma concentration-time profiles of quercetin and its conjugates after oral and intravenous administration.
Results. Only 5.3% of unchanged quercetin was bioavailable, although the total quercetin absorbed was as high as 59.1%. After oral administration, about 93.3% of quercetin was metabolized in the gut, with only 3.1% metabolized in the liver. No significant enterohepatic recirculation was observed for both quercetin and its conjugated metabolites. The pharmacokinetic model fitted well the observed data of quercetin and its conjugates.
Conclusions. Our study clarifies the relative importance of the gut, liver, and bile in the metabolism and excretion of quercetin and its conjugates. The pharmacokinetic model appears to be suitable for describing the absorption and disposition of the quercetin and its conjugates and may be applicable to other flavonoids that undergo similar pharmacokinetic pathways.

KEY WORDS: absorption, gut and liver first-pass effect; metabolism; pharmacokinetic model; quercetin.

INTRODUCTION

Flavonoids are a group of polyphenolic compounds widely present in plants and vegetables, such as onion, apple, tea, and *Ginkgo biloba*. These products are commonly consumed as food and medicine (1–3). Flavonoids or flavonoid-containing products have been reported to possess extensive biological activities, including antioxidative and anticancer properties (3,4). Epidemiological studies also have shown that high intake of flavonoids is associated with reduced risk of coronary heart disease and cancers (4,5). Thus, flavonoid-containing products may be beneficial when consumed as health food or herbal supplements.

Quercetin (3,5,7,3′,4′-pentahydroxyflavanone) is one of the most prevalent flavonoids present in health food or herbal products. Besides its antioxidative and anticancer properties, quercetin also has been reported to benefit prostatitis and interstitial cystitis (6,7). In view of the popular usage of quercetin containing products and the potential of quercetin as a promising pharmacological agent, the pharmacokinetics and pharmacodynamics of quercetin should be carefully studied.

At present, the pharmacokinetics of quercetin has not been fully characterized, although a number of studies have been carried out both in animals and humans. These studies showed that the oral bioavailability of the unchanged quercetin is low. However, high amount of metabolites, for example, conjugated quercetin is found in the systemic circulation (8,9). The low bioavailability of quercetin and high metabolite concentrations indicate extensive gut and/or liver first-pass metabolism (9,10). The relative contribution of gut *versus* liver is nevertheless unknown. Additionally, the high concentration of conjugated quercetin observed in the bile indicates potential enterohepatic recirculation (2,11), which may contribute to the high plasma metabolite concentrations in the body. The relationship of the biliary excretion or enterohepatic recirculation toward gut and liver first-pass effect is unknown at present.

In view of the lack of mechanistic and quantitative description of quercetin and its metabolites, this study is designed to 1) determine the relative contribution of gut and liver first-pass effect of quercetin, 2) clarify the significance of enterohepatic recirculation, and 3) develop a pharmacokinetic model that can simultaneously describe the pharmacokinetics of both the unchanged quercetin and its conjugated metabolites following oral and intravenous administration of quercetin.

[1] School of Pharmacy, The Chinese University of Hong Kong, Shatin, NT, Hong Kong.
[2] Present address: Department of Pharmacy, The First Affiliated Hospital, Sun Yat-sen University, Guangzhou, China.
[3] To whom correspondence should be addressed. (e-mail: msschow@cuhk.edu.hk)

MATERIALS AND METHODS

Materials

Quercetin, fisetin (internal standard), and β-glucuronidase/sulfatase (type H-1, *Helix pomatia*) were purchased from Sigma (St. Louis, MO, USA). Isorhamnetin was obtained from Indofine Chemical Company, Inc. (Somerville, NJ, USA). Hydroxypropyl-β-cyclodextrin [HP-β-CD, molar substitution (M.S. = 0.6)] was purchased from Sigma (St. Louis, MO, USA). Waters Oasis Hydrophilic-Lipophilic-Balanced (HLB, 1cc) copolymer extraction cartridges were purchased from Waters (Milford, MA, USA). HPLC grade methanol and acetonitrile were purchased from Labscan Asia Co. Ltd. (Bangkok, Thailand).

Animals

Male Sprague-Dawley rats, weighing 280–330 g, were obtained from Laboratory for Animal Services Centre, The Chinese University of Hong Kong. The rats were housed in metabolic cages under a 12/12 h light/dark cycle (with lights coming on at 7 a.m. and turning off at 7 p.m.). The rats were fed with rice as described previously (12). Ethical approval for the study was obtained from the Animal Care and Ethics Committee of The Chinese University of Hong Kong.

Methods

Determination of First-Pass Effect in the Gut and Liver

To distinguish the first-pass effect of gut *versus* liver, oral, intraportal as well as intravenous quercetin were administered separately in three groups of rats ($n = 5$ in each group). Group 1 received a single *iv* dose of 10 mg/kg of quercetin via a jugular vein. Group 2 received the same dose orally by gavage. Group 3 received the same dose by intraportal injection. The quercetin dose was prepared as in 15% (w/v) HP-β-CD water solution. For drug administration and sampling, the jugular and portal polyethylene catheters (0.40 mm I.D., 0.80 mm O.D., Portex Ltd., Hythe, Kent, England) were inserted using the technique as previously described (13). Following each dose (single *iv* and intraportal injection administration was finished about 10 s), a 220 μl of blood was withdrawn from the right jugular vein at 1, 3, 5, 8, 12, 16, 20, 25, 30 min for the determination of unchanged quercetin concentration. Also, a 50 μl of blood was collected at 1, 5, 12, 30 min and 1, 2, 4, 8, 12, 24 h for the determination of total quercetin concentration. After each sampling, the blood loss was replaced with an equal volume of normal saline. The blood sample was centrifuged at 13,000 rpm for five minutes; then the plasma was separated and stored at −80°C until analysis.

Following the *iv* and oral dosing, urine was collected at 0–0.5, 0.5–1, 1–2, 2–4, 4–8, 8–12, 12–18, 18–24 h intervals and stored in tubes containing 0.5 ml concentrated acetic acid to maintain urinary pH below 3.0 (to prevent degradation of quercetin). Feces was also collected over 24 h. All urine and feces samples were stored at −80°C until analysis.

Evaluation of Biliary Excretion and Enterohepatic Recirculation of Quercetin

Assessment of Biliary Excretion. Biliary excretion was determined in bile duct cannulated rats ($n = 4$). The bile duct cannulation was performed according to the method reported previously (14). Following an intravenous dose of 10 mg/kg quercetin, the bile samples were collected right before (time zero) and at 0–0.25, 0.25–0.5, 0.5–1, 1–2, 2–4, 4–8, 8–12, 12–18, 18–24 h intervals post dosing. Also blood samples were collected as described previously. All bile and plasma samples were stored at −80°C prior to analysis.

Evaluation of Reabsorption of Quercetin from the Rat Gut in a Linked-Rat Model. To study the enterohepatic recirculation of quercetin, a linked-rat model (15) was used. In the linked-rat model, paired-rats (one for donor and the other for recipient of bile) were anesthetized by intraperitoneal injection of sodium pentobarbital (50 mg/kg). The bile of the donor rat was channeled to flow into the corresponding duodenum of the recipient rat according to a method described previously (15).

In 3 pair of rats, a 10 mg/kg dose of quercetin in 15% (w/v) HP-β-CD water solution was administered intravenously to each donor rat. A 220 μl blood sample was collected from the portal vein of each recipient rat at 0, 2, 5, 10, 15, 20, 25, 30 min and 1, 2, 4, 8 h post drug administration. After each sampling, the blood loss was supplemented with an equal volume of normal saline. The plasma was separated from the blood and then stored at −80°C until analysis.

Evaluation of Reabsorption of Quercetin from the Rat Gut by Administration of Bile Containing Quercetin and its Metabolites. Because the rats in the linked-rat study were carried out under anesthesia which may influence the drug absorption (16), enterohepatic recirculation of quercetin was further investigated by the oral administration of bile that contained quercetin and its metabolites. Following an *iv* administration of a 10 mg/kg dose of quercetin to three rats, the bile that contained quercetin and its metabolites were collected continuously over two hours via a bile duct catheter (in a prior experiment, it was found that more than 90% of quercetin was excreted in the bile within 2 h). The bile collected from each of the 3 rats was then administered to another three rats by intragastric gavage (1 ml), followed by flushing with 0.5 ml water (Observation was made to encertain that no disgorge occurred during experiment). A 220 μl blood sample was collected via a portal vein catheter at 0, 2, 5, 10, 15, 20, 25, 30 min, and then 50 μl blood collected at 1, 2, 4, 8 h. The blood loss was replaced with an equal volume of normal saline. The plasma was separated from the blood by centrifugation at 13000 rpm for 5 min, and then stored at −80°C until analysis.

Determination of Absorption Rate Constant

The absorption rate constant of quercetin was determined and calculated according to the method previously described (17). This method assumes that there is no difference in the portal and systemic plasma drug concentration after the *iv* administration. The lack of portal-systemic concentration difference after *iv* administration was subsequently verified

in 5 rats. Thus, any increase in portal plasma concentration following oral drug administration is presumed to be due to absorption, and the absorption rate constant can be estimated by measuring the portal-systemic concentration gradient. The portal-systemic concentration difference after oral administration was determined at 2, 5, 10, 15, 20, 25, 30, 35, 40, 45 min and 1, 2, 4, 8 h (n = 5).

Assay of Quercetin and Metabolites

The plasma concentrations of unchanged free and total quercetin in rat plasma, urine or bile were determined by an HPLC method with electrochemical detection. The chromatographic system consisted of a Waters 2695 separation module, and a Waters 464 Electrochemical Detector (ECD) with a glassy carbon working electrode and an Ag/AgCl reference electrode (Milford, MA, USA). The working potential of ECD was set at +1.2 V *vs.* Ag/AgCl. Chromatographic separation was achieved by a reversed-phase C_{18} column (Hypersil BDS C_{18}, 5 μm, 250 × 4.6 mm I.D., Runcorn, Cheshire, UK) attached to a guard column (Hypersil BDS C_{18}, 5 μm, 10 × 4.6 mm I.D.). The mobile phase, consisting of a mixture of methanol (0–15 min: 5–80%), acetonitrile (0–15 min: 25–0%) and phosphate buffer (pH 2.5) (0–15 min: 70–20%) was run with a gradient elution program.

For the determination of unchanged quercetin, 10 μl of acetic acid (0.58 M) and 10 μl of ascorbic acid solution (1 M) were added to 0.1 ml of plasma sample, followed by the addition of 10 μl of internal standard (fisetin, 5 μg/ml). The mixture was then diluted with 1 ml of 30% methanol in 0.05 M sodium dihydrogen orthophosphate buffer (pH 2.4, adjusted by phosphate acid). After vortexing and centrifugation, the supernatant was applied to a HLB cartridge [which was preconditioned with 1 ml of methanol, followed by 1 ml of 0.05 M sodium dihydrogen orthophosphate buffer (pH 2.5)]. After rinsing the cartridge with 1 ml 80% methanol in 0.05 M sodium dihydrogen orthophosphate buffer (pH 2.5), targeted compounds were eluted from the cartridge using 1 ml methanol. The eluate was evaporated to dryness under a gentle stream of nitrogen. The residue was reconstituted in 100 μl of 50% methanol in the 0.05 M sodium dihydrogen orthophosphate buffer (pH 2.5), and 50 μl was injected into HPLC.

For the determination of total quercetin in plasma, a 20 μl of plasma was hydrolyzed by β-glucuronidase/sulfatase (5000 units/ml, dissolved in 0.2 M sodium acetate buffer, pH 5.0) according to the procedure described previously (18). After hydroxylation, the sample was extracted in the same manner as described above.

The concentrations in the bile and urine were measured using the same method as the plasma (These bile samples were first centrifuged and then diluted 10 fold with blank bile before extraction). Fecal samples were extracted with 200 ml methanol by shaking vigorously for 5 min. A 1 ml methanol extraction suspension was transferred to a clean tube and evaporated to dryness. The sample was then analyzed using the same method as the plasma.

The calibration curve was linear in the examined concentration range of 0.01 to 50 μg/ml ($R^2 \geq 0.998$) with the detection limit of 10 ng/ml. The inter-day and intra-day precisions were less than 15%. The extraction recoveries were 65%~80% for all samples.

Pharmacokinetic Data Analysis

Pharmacokinetic analyses were performed using the non-compartmental analysis as well as compartmental pharmacokinetic modeling. For non-compartmental analysis, the area under the concentration-time (AUC) curve was calculated using linear/log trapezoidal method (WinNonlin software package, version 2.1, Pharsight Corporation, Palo Alto, CA, USA). The oral bioavailability (F) relative to intravenous injection was calculated as $F = (AUC_{po}/AUC_{iv}) \times 100\%$.

Pharmacokinetic Model Construction and Validation. The proposed model is shown in Fig. 1. Following a given oral dose, quercetin can be divided into three fractions. Fraction 1 (F_1) represents the directly absorbed quercetin, fraction 2 (F_2) represents the conjugated quercetin in the gut lumen or gut wall which is subsequently absorbed via portal vein; and fraction 3 (F_3), represents the degraded product in the gut lumen or gut wall which are excreted. Once quercetin (F_1) is absorbed, it is conjugated by the liver or excreted via urine/bile. Once the conjugated metabolites (F_2) is absorbed, it is excreted in the urine or bile.

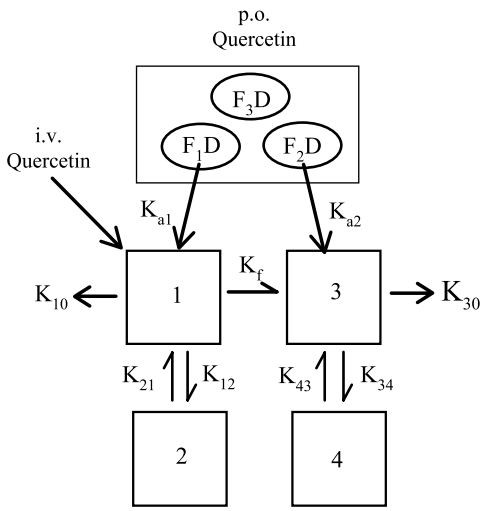

Fig. 1. Schematic representation of the compartmental model for unchanged quercetin and its glucuronide/sulfate conjugates following oral and *iv* administration in rats. Compartments are as follows: 1 and 2 represent central and peripheral compartments of quercetin; 3 and 4 represent central and peripheral compartments of quercetin glucuronide/sulfate metabolites. K_f is the constant of metabolic conversion to (or formation of) glucuronide/sulfate conjugates; K_{10} is the excretion rate constant of unchanged quercetin in urine or bile; K_{12}, K_{21}, K_{34}, and K_{43} are the intercompartmental rate constants; K_{30} is the elimination rate constant of quercetin glucuronide/sulfate metabolites through biliary excretion and/or further degradation, for example, to CO_2 (see "Discussion"); K_{a1} and K_{a2} are the oral absorption rate constants of quercetin and quercetin glucuronide/sulfate conjugates, respectively. D is the oral dose; F_1 is the absorbed fraction of quercetin; F_2 is the absorbed fraction of quercetin glucuronide/sulfate conjugates; F_3 is the unabsorbed and degraded fraction in the gut (see "Discussion").

Assumptions for this model are 1) rapid conversion of unchanged quercetin to its glucuronide/sulfate conjugates in the gut; 2) quercetin glucuronide/sulfate conjugates are the major metabolites of quercetin in rats and the minor quercetin methylate conjugates are not significant and can be ignored; 3) glucuronide/sulfate conjugates are combined as one entity; 4) the linear pharmacokinetics of the unchanged quercetin and its metabolites (which were observed at doses of 25 mg/kg and 50 mg/kg in rats) (19).

The differential equations for the change of amount of substance with time in each compartment following oral and *iv* doses are shown in the Appendix. As a part of model validation, structurally identification analysis was first performed to assure all proposed model parameters could be practically determined. Based on the results of identification analysis, the integrated solutions for the plasma concentrations of quercetin and its conjugates were subsequently obtained (see Appendix).

Model Fitting and Validation. The proposed model was fitted to the combined mean plasma concentration data of unchanged quercetin and its conjugates after oral and *iv* administration. Nonlinear regression analysis was performed using Gauss-Newton method, with the aid of WinNonlin software package (version 2.1, Pharsight Corporation, Mountain View, CA, USA). Weighted sum of squared residuals (WSSR) was used as the objective function.

In view of the wide plasma concentration range of unchanged quercetin and its conjugates, different weighting schemes (i.e., weighting factor of 1, 1/C, $1/C^2$) were firstly investigated for the model fitting. The use of a weighting factor of $1/C^2$ was found to be most appropriate based on the residual plot and lowest value of WSSR. In addition, the initial evaluation of the model also demonstrated that the incorporation of a lag-time (t_{lag}) improved the model fitting and thus was subsequently used for all model fitting following oral administration.

Initial parameter estimates for V_1, K_{21}, α_1, β_1 were obtained from the two-compartmental analysis of the *iv* quercetin concentration data. Initial estimates for F_1, F_2, K_{a1}, and K_{a2} were obtained using the experimental data (see result tables). β_2 was estimated by linear-regression of the terminal phase of the concentration-time curve of glucuronide/sulfate conjugates. Initial estimates for the remaining parameters (V_3, K_{43}, α_2) were arbitrarily set at a range for iteration.

The goodness-of-fit was assessed by visual inspection of the residual plots, parameter estimation precision, correlation (R) between the observed and predicted concentration values, Akaike's information criterion (AIC) and Schwarz criteria (SC). In addition, the predictive performance of this model was also evaluated according to the criteria suggested by Sheiner *et al.* (20). The mean error (ME) and the root mean square prediction error (RMSE) were estimated according to the following:

$$\mathrm{ME} = \frac{\sum_{i=1}^{n} (\text{predicted value} - \text{observed value})}{n}$$

$$\mathrm{RMSE} = \sqrt{\frac{\sum_{i=1}^{n} (\text{predicted value} - \text{observed value})^2}{n}}$$

RESULTS

First-Pass Effect of Quercetin in the Gut and Liver

The plasma concentration–time profiles of unchanged and total quercetin following *iv* and oral adminsitraiton are shown in Fig. 2. The systemic bioavailability of oral quercetin based on the unchanged quercetin, the combined glucuronide/sulfate conjugates and total quercetin were 5.3%, 47.8% and 59.1%, respectively (see Table III). After oral administration, about 6.7% of oral dose was absorbed into portal vein in the form of unchanged quercetin. Thus, about 93.3% of oral quercetin dose was "lost" in the gut.

The bioavailability of unchanged quercetin following intraportal administration was 52.6%, which corresponded to the hepatic extraction ratio of 47.4%. However, only 3.1% of an oral dose was found to be extracted by the liver following the intestinal first-pass. The AUCs of total quercetin following intraportal and intravenous administration of quercetin were similar (mean ± SD, 20.44 ± 5.1 and 23.31 ± 2.96 μg h/ml, unpaired student *t*-test, $p > 0.05$), indicating that there was no significant conversion to metabolites other than quercetin glucuronide or sulfate following intraportal administration.

Bilary Excretion and Enterohepatic Recirculation

The main forms of quercetin excreted in the rat bile were its glucuronide/sulfate and methylate conjugates; unchanged

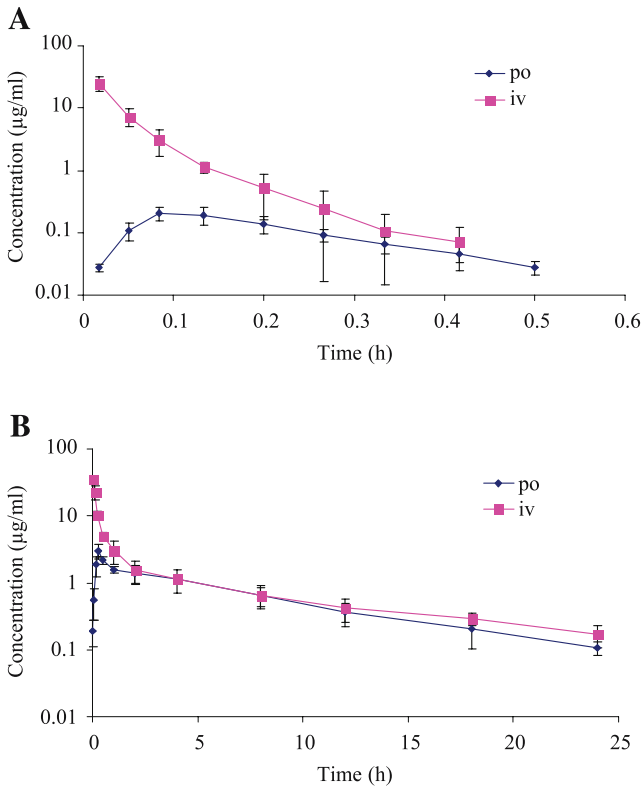

Fig. 2. Plasma concentration of unchanged (A) and total (B) quercetin after an oral or *iv* administration of 10 mg/kg quercetin to rats (n = 5). Error bar refers to the standard deviation of concentration data at each sampling time point.

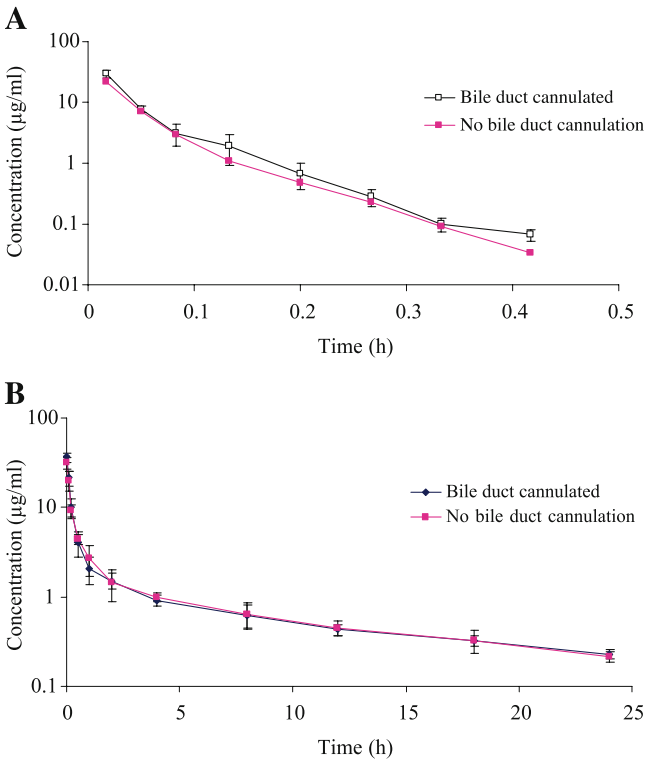

Fig. 3. Plasma concentration of unchanged (A) and total (B) quercetin following *iv* administration of 10 mg/kg quercetin to rats with or without bile duct cannulation. ($n = 4$). Error bar refers to the standard deviation of concentration data at each sampling time point.

quercetin was not detected. As much as 35% of a quercetin dose was recovered from the bile as the conjugates.

The studies on enterohepatic recirculation indicated that such recirculation was unlikely: First of all, the plasma concentration profiles of both unchanged quercetin and total quercetin were found to be superimposable in rats with and without bile duct cannulation (Fig. 3). Second, in the linked-rat model, quercetin was detected in the portal vein of the recipient rat only as a trace amount of total quercetin at 6 h post-dosing. Thirdly, following the intra-gastric administration of bile containing quercetin metabolites, only a trace amount of total quercetin was observed in the portal vein during the 8 h experiment.

Absorption Rate Constants and Urinary and Fecal Excretion

The absorption rate constants of unchanged quercetin and quercetin glucuronide/sulfate conjugates were calculated to be 5.32 h^{-1} and 0.83 h^{-1}, respectively. Urinary and fecal excretion were low (about 5%).

Model Fitting and Validation

The plasma concentration-time data of both unchanged quercetin and quercetin glucuronide/sulfate conjugates following either oral or *iv* administration were well described by the proposed model (Table I; Fig. 4).

The estimated pharmacokinetic parameters are summarized in Table II, III. The coefficient of variation (CV%) of the parameter estimates were all less than 30%, and the 95% confidence intervals were generally small for all the parameters.

Model identifiability analysis indicated that the model parameters were identifiable (see Appendix). The noncompartmental parameters such as C_{max}, t_{max}, $AUC_{0-\infty}$ estimated by the model were also comparable to those calculated by the non-compartmental method.

DISCUSSION

Quercetin is a representative polyphenolic compound that has low bioavailability of the unchanged form but high bioavailability of the conjugated form. The present animal study clarifies the relative contribution of first-pass effect of quercetin in the gut *versus* liver, two important factors responsible for the low bioavailability. Also the study confirms the lack of enterohepatic recirculation of quercetin and its conjugates. Based on these results, a specific pharmacokinetic model for describing quercetin and its active glucuronide/sulfate conjugates in the body has been developed which not only is applicable to quercetin but mostly likely to other polyphenolic compounds.

Our model provided structurally identifiable parameters with good precision. The coefficient variation of the parameter estimates ranged from 6.5% to 27%. The values of C_{max}, t_{max}, and AUC estimated by this model are also close to those calculated by the non-compartmental method. These results

Table I. Goodness of Fit

	WSSR	R	ME	RMSE	AIC	SC
Intravenous dose						
Unchanged quercetin	0.4506	0.9998	−0.0214	0.1494		
Glucuronide/sulfate conjugates	0.4307	0.9674	−0.1711	0.5612		
Oral dose						
Unchanged quercetin	0.1267	0.9542	0.0041	0.0216		
Glucuronide/sulfate conjugates	0.6236	0.9309	−0.068	0.1967		
All curves combined	1.226				34.15	56.1

WSSR = Weighted sum of squared residuals.
R = Correlation coefficient between the observed and predicted values.
AIC = Akaike's information criterion.
SC = Schwarz criteria.
ME = Mean error.
RMSE = The root mean square prediction error.

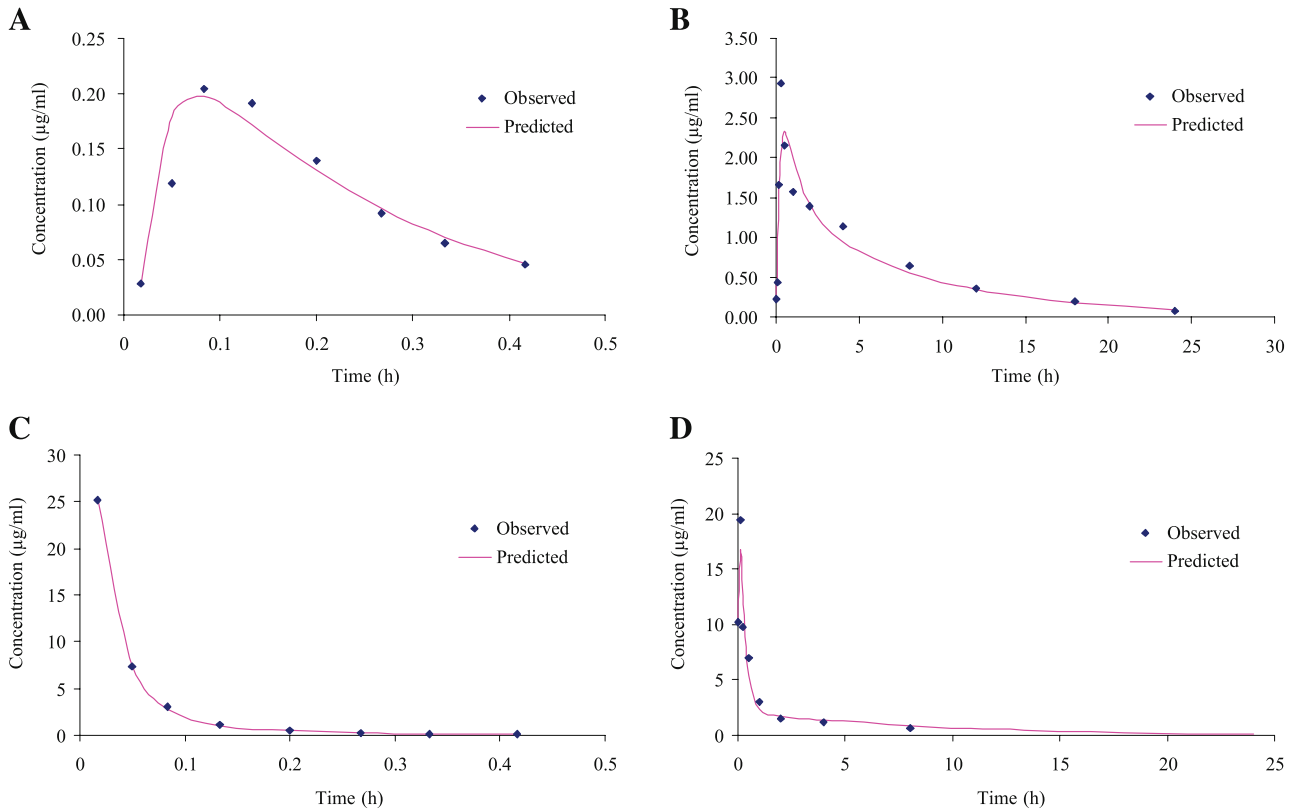

Fig. 4. Model fitting to the unchanged (A) and conjugated (B) plasma quercetin concentration-time profile following oral administration, as well as the unchanged (C) and conjugated (D) plasma quercetin concentration-time profile following *iv* administration.

suggest that the proposed model is reliable for describing the concentration-time profiles of both the unchanged quercetin and its glucuronide/sulfate conjugates.

A concern in the current study may be the determination of the combined conjugates of quercetin instead of each separately. However, there are three reasons for our interest in the combined conjugates: 1) the combined conjugates represent the dominant metabolites of quercetin metabolism (10,21). 2) The combined glucuronide/sulfate conjugates have been shown to possess antioxidative activity, with potency being half of that of free quercetin (22–23). 3) The combined conjugates have been identified also in the human blood with similar elimination half-life and renal clearance after administration of different quercetin products (8). Thus, the combined conjugate concentration can represent a meaningful entity for pharmacokinetic and pharmacodynamic studies.

Our studies did not identify carbon dioxide as a metabolite, although it was found to be produced from the fission of the pyron ring of quercetin in the digestive tract (24). The previous study data (24) suggested that CO_2 was usually a degraded product from quercetin or its conjugates in the gut, and it could be absorbed, circulated and then expired via the lung. In our pharmacokinetic model, we considered CO_2 as part of the degraded products (as represented by F_3D plus that following biliary excretion of the conjugates through K_{30} (see Fig. 1).

Our studies did not found any significant enterohepatic recirculation of quercetin and its conjugates although such recirculation was proposed previously due to its high biliary excretion (2,11). The reasons for the lack of enterohepatic recirculation of quercetin or its metabolites may be related to their conversion to CO_2 in the gut lumen by microflora (24).

Although enteric recycling was reported (11), it does not affect our modeling, because we have already taken into account all the produced or enteric recycling quercetin/conjugated metabolites that are absorbed from gut compartment to central compartment in our model (as F_1 and F_2).

Only small amount of quercetin was founded to be eliminated in the urine and feces in our study. This is consistent with the observations by others who determine urinary and fecal as unchanged quercetin or total quercetin. Gugler *et al.* (25) found that after intravenous administration of a 100 mg quercetin, only 0.65% of the dose was recovered in the form of unchanged quercetin, while 7.4% of the dose was excreted in the urine in the form of conjugated metabolite of quercetin. In a phase I clinical trial of quercetin (in fifty-one cancer patients) at doses of 60 to 2000 mg/m^2, the percentage of quercetin in urine over 24 h ranged from 0.03% to 7.6% (26). The recovery from feces was only 1.5–5.0% after an intravenous dose (0.3 mg ^{14}C-quercetin) in the study by Walle *et al.* (27). However, higher urinary excretion of radiolabeled quercetin was reported in human (18.4~26.8%) (26) and in rat (16.5 ± 7%, mean ± SD) (24) which may be due to the degradation products of quercetin or its conjugates (28). Therefore, urinary and fecal elimination of quercetin are not the main excretion routes in human subjects or in rats.

In this study, our proposed are a specific two-compartment model linking the parent drug (unchanged quercetin)

Table II. Parameter Estimates Obtained by Simultaneous Fitting of the Model to the Mean Plasma Concentrations of Unchanged Quercetin and Glucuronide/Sulfate Conjugates Following *iv* and Oral Administration

Parameter	Estimate	SE	CV%	95% Confidence interval	
F_1(%)	0.04	0.01	15.76	0.03	0.05
V_1 (L/kg)	0.23	0.06	27.10	0.10	0.36
K_{a1} (h^{-1})	5.74	0.62	10.90	4.45	7.02
K_{21} (h^{-1})	12.19	2.38	19.53	7.30	17.06
K_{12} (h^{-1})	5.24[a]				
α_1 (h^{-1})	39.36	7.66	19.47	23.63	55.08
β_1 (h^{-1})	9.84	1.30	13.17	7.18	12.50
K_f (h^{-1})	31.77[a]				
F_2(%)	0.51	0.05	10.92	0.39	0.62
V_3 (L/kg)	0.41	0.06	14.70	0.28	0.53
K_{a2} (h^{-1})	0.85	0.18	20.94	0.48	1.21
K_{43} (h^{-1})	0.34	0.06	17.81	0.21	0.46
K_{34} (h^{-1})	2.24				
α_2 (h^{-1})	3.38	0.53	15.72	2.29	4.47
β_2(h^{-1})	0.09	0.01	9.83	0.07	0.11
K_{30} (h^{-1})	0.89[a]				
t_{lag} (h)	0.014	0.001	6.48	0.012	0.016

F_1 = fraction of dose which is absorbed as unchanged quercetin.
F_2 = fraction of dose which is converted in the gut and subsequently reaches the systemic circulation as glucuronide/sulfate conjugates.
V_1 and V_3 = volume of compartment 1 and 3.
K_{a1} and K_{a2} = absorption rate constant of unchanged quercetin and glucuronide/sulfate conjugates.
K_f = biotransformation rate constant of unchanged quercetin.
K_{30} = elimination rate constant of quercetin glucuronide/sulfate conjugates.
α, β = Exponent of the polyexponential equation.
t_{lag} = absorption lag time.
K_{12}, K_{21}, K_{34}, K_{43} = inter-compartmen transfer rate constant.
[a] K_{12}, K_f, K_{34} and K_{30} are secondary parameters calculated by equations 40–43.

and its metabolites (glucuronide/sulfate conjugates). This model allows simultaneous fitting of all these concentrations in different compartments. Such a model will be useful for planning future pharmacokinetic-pharmacodynamic studies and subsequent delineation of the conjugates' contribution to the overall pharmacodynamic effects of quercetin. As many flavonoids (e.g., kaempferol, morin, luteolin) manifest similar *in vivo* metabolic fate and pharmacokinetic characteristics as quercetin, this proposed model can be potentially useful to describe these flavanoids. In view of the popular use of flavonoids, their pharmacokinetic data will provide scientific basis in the development of herbal products that contain these compounds.

Although our rat pharmacokinetic model may be clinically applicable due to the similarity of great majority of the pharmacokinetic parameters (bioavailability, distribution volume, metabolism, excretion and half life of unchanged quercetin and total quercetin) observed between rat and human (8,10,19,24–27,29–31), more human studies are desirable to confirm the applicability of this model.

In summary, the current study clarifies the absorption and disposition of quercetin as well as the importance of the gut, liver and bile in the metabolism and excretion of quercetin and its conjugates. These data allows generation of a specific pharmacokinetic model which can simultaneously describe the plasma concentration-time profiles of unchanged quercetin and its glucuronide/sulfate conjugates. This model can be potentially applicable to many other flavonoids which undergo similar pharmacokinetic pathways.

APPENDIX

Mass Balance of Each Compartment

The differential equations for the change of amount $\left(\frac{dX}{dt}\right)$ of substance with time in each compartment following an *iv* dose are shown as follows:

$$\frac{dX_1}{dt} = -\left(K_{12} + K_f + K_{10}\right)X_1 + K_{21}X_2 \quad \text{(A1)}$$

$$\frac{dX_2}{dt} = K_{12}X_1 - K_{21}X_2 \quad \text{(A2)}$$

$$\frac{dX_3}{dt} = K_fX_1 - (K_{34}+K_{30})X_3 + K_{43}X_4 \quad \text{(A3)}$$

$$\frac{dX_4}{dt} = K_{34}X_3 - K_{43}X_4 \quad \text{(A4)}$$

where $\frac{dX_1}{dt}$, $\frac{dX_2}{dt}$, $\frac{dX_3}{dt}$, and $\frac{dX_4}{dt}$ are the change of amount of substance with time in compartments 1, 2, 3, and 4 respectively, and other terms have been described previously.

Table III. Comparison of Pharmacokinetic Parameters Obtained by the Model and Non-Compartmental Model

	Proposed model				Non-compartmental model			
	t_{max} (h)	C_{max} (μg/ml)	$AUC_{0-\infty}$ (h*μg/ml)	Bioavailability (%)	t_{max} (h)	C_{max} (μg/ml)	$AUC_{0-\infty}$ (h*μg/ml)	Bioavailability (%)
Intravenous dose								
Unchanged quercetin	0	48.72	1.13				1.13	
Glucuronide/sulfate conjugates	0.084	17.27	27.08		0.083	19.38	30.58	
Oral dose								
Unchanged quercetin	0.078	0.21	0.06	5.3	0.083	0.2	0.06	5.3
Glucuronide/sulfate conjugates	0.42	2.53	15.1	55.8	0.27	2.93	14.63	47.8

The differential equations for this model with an oral dose are shown as follows:

$$\frac{dX_{g1}+dX_{g2}}{dt} = -\left(K_{a1}X_{g1} + K_{a2}X_{g2}\right) \tag{A5}$$

$$\frac{dX_1}{dt} = K_{a1}X_{g1} - \left(K_{12} + K_f + K_{10}\right)X_1 + K_{21}X_2 \tag{A6}$$

$$\frac{dX_2}{dt} = K_{12}X_1 - K_{21}X_2 \tag{A7}$$

$$\frac{dX_3}{dt} = K_{a2}X_{g2} + K_fX_1 - (K_{34} + K_{30})X_3 + K_{43}X_4 \tag{A8}$$

$$\frac{dX_4}{dt} = K_{34}X_3 - K_{43}X_4 \tag{A9}$$

where $\frac{dX_{g1}}{dt}$ and $\frac{dX_{g2}}{dt}$ are the change of amount of substance with time in the gut for the parent drug and metabolites to be absorbed, so that at time 0, X_{g1} and X_{g2} equal to F_1D_0 and F_2D_0 respectively (see Fig. 1); all other terms have been defined previously.

Model Identifiability Analysis

To test the validity of this model (i.e. to test whether the model parameters can be practically identified), structural identifiability analysis was performed using the similarity transformation approach (32).

Generally, a linear system can be described as:

$$\frac{dx}{dt} = A(p)x + B(p)u, x(t_0) = x_0(p) \tag{A10}$$

$$y = C(p)x \tag{A11}$$

where A is the $(n \times n)$ system matrix, B is the input matrix, and C is the output matrix, x_0 represents the initial condition and p represents the unknown parameter in these matrices.

The similarity transformation approach utilizes the fact that for another model characterized as $(\bar{A}, \bar{B}, \bar{C})$, it is necessary and sufficient that there exists a nonsingular matrix T such that:

$$T\bar{B} = B \tag{A12}$$

$$\bar{C} = CT \tag{A13}$$

$$T\bar{A} = AT \tag{A14}$$

That is, if solving Eqs. (A12)–(A14) yields the solution that T is the $n \times n$ identity matrix, the model is then globally identifiable.

For the model described in Fig. 1, structural identifiability analysis was performed under the condition that both *iv* and oral doses of quercetin were administered, and the plasma concentrations of unchanged quercetin and its combined glucuronide/sulfate conjugates were measured.

The matrixes of the model are as follows:

$$A = \begin{pmatrix} -(K_{a1}+K_{a2}) & 0 & 0 & 0 & 0 \\ K_{a1} & -(K_{12}+K_f+K_{10}) & K_{21} & 0 & 0 \\ 0 & K_{12} & -K_{21} & 0 & 0 \\ K_{a2} & K_f & 0 & -(K_{34}+K_{30}) & K_{43} \\ 0 & 0 & 0 & K_{34} & -K_{43} \end{pmatrix} \tag{A15}$$

$$B = \begin{pmatrix} 1 & 0 \\ 0 & 1 \\ 0 & 0 \\ 0 & 0 \\ 0 & 0 \end{pmatrix} \tag{A16}$$

$$C = \begin{pmatrix} 0 & \frac{1}{V_1} & 0 & 0 & 0 \\ 0 & 0 & 0 & 0 & \frac{1}{V_3} \end{pmatrix} \tag{A17}$$

where V_1 and V_3 are the volumes of compartment 1 and 3, respectively.

Let P be the vector of the unknown parameters, and T be a 5×5 matrix $P \in [K_{a1}, K_{a2}, V_1, V_3, K_{12}, K_{21}, K_{10}, K_f, K_{34}, K_{43}, K_{30}]$

$$T = \begin{pmatrix} t_{11} & t_{12} & t_{13} & t_{14} & t_{15} \\ t_{21} & t_{22} & t_{23} & t_{24} & t_{25} \\ t_{31} & t_{32} & t_{33} & t_{34} & t_{35} \\ t_{41} & t_{42} & t_{43} & t_{44} & t_{45} \\ t_{51} & t_{52} & t_{53} & t_{54} & t_{55} \end{pmatrix} \tag{A18}$$

By substituting A, B, C, and T into Eqs. (A12)–(A14) gives the following results: 1) V_1, K_{a1}, K_{12}, K_{21}, K_{34}, K_{43}, and K_{30} are identifiable, whereas K_{a2}, K_f, K_{1e} and V_3 are not identifiable; 2) if V_3 is known *a priori*, K_{a2}, K_f, and K_{1e} could be identifiable. Alternatively, if K_{1e} can be assumed to be zero, then the remaining parameters K_f, K_{a2}, and V_2 will be identifiable.

Our previous studies in rats showed that the unchanged quercetin in the systemic circulation is primarily metabolized to glucuronide/sulfate conjugates, and only small amount of quercetin (less than 1%) was excreted into the urine and bile. Thus it is reasonable to assume that the excretion pathway of the unchanged quercetin be ignored (i.e., $K_{10} = 0$). With this assumption, the proposed model is globally identifiable and all the parameters can be identifiable when both *iv* and oral doses are administered.

Integrated Solutions for the Plasma Concentrations of Unchanged Quercetin and Glucuronide/Sulfate Conjugates

With an assumption of $K_{10} = 0$, solving Eqs. (A1)–(A4) with initial conditions (at time $t = 0$, $X_{1(0)} = D$, $X_{2(0)} = X_{3(0)} = X_{4(0)} = 0$), the plasma concentration of unchanged quercetin in compartment 1, C_1(t), and its glucuronide/sulfate conju-

gates in compartment 3, $C_3(t)$, at any time after an *iv* administration can be expressed by (Eqs. (A19) and (A20)):

$$C_1(t) = \frac{D}{V_1} \cdot \left[\frac{k_{21} - \alpha_1}{\beta_1 - \alpha_1} e^{-\alpha_1 t} + \frac{K_{21} - \beta_1}{\alpha_1 - \beta_1} e^{-\beta_1 t}\right] \quad \text{(A19)}$$

$$C_3(t) = \frac{DK_f}{V_3} \cdot \left[\lambda_1 e^{-\alpha_1 t} + \lambda_2 e^{-\beta_1 t} + \lambda_3 e^{-\alpha_2 t} + \lambda_4 e^{-\beta_2 t}\right] \quad \text{(A20)}$$

$$\text{where } \lambda_1 = \frac{(K_{21} - \alpha_1)(K_{43} - \alpha_1)}{(\beta_1 - \alpha_1)(\alpha_2 - \alpha_1)(\beta_2 - \alpha_1)} \quad \text{(A21)}$$

where

$$\lambda_2 = \frac{(K_{21} - \beta_1)(K_{43} - \beta_1)}{(\alpha_1 - \beta_1)(\alpha_2 - \beta_1)(\beta_2 - \beta_1)} \quad \text{(A22)}$$

$$\lambda_3 = \frac{(K_{21} - \alpha_2)(K_{43} - \alpha_2)}{(\alpha_1 - \alpha_2)(\beta_1 - \alpha_2)(\beta_2 - \alpha_2)} \quad \text{(A23)}$$

$$\lambda_4 = \frac{(K_{21} - \beta_2)(K_{43} - \beta_2)}{(\alpha_1 - \beta_2)(\beta_1 - \beta_2)(\alpha_2 - \beta_2)} \quad \text{(A24)}$$

$$\alpha_1 + \beta_1 = K_f + K_{12} + K_{21} \quad \text{(A25)}$$

$$\alpha_1 \beta_1 = K_f K_{21} \quad \text{(A26)}$$

$$\alpha_2 + \beta_2 = K_{30} + K_{34} + K_{43} \quad \text{(A27)}$$

$$\alpha_2 \beta_2 = K_{30} K_{43} \quad \text{(A28)}$$

In the above Eqs. (A19)–(A28), D is the dose given intravenously, t is the time after *iv* administration, α_1 and β_1 are the first-order hybrid rate constants for the distribution and elimination phases for unchanged quercetin, respectively; whereas α_2 and β_2 are the first-order hybrid rate constants for the distribution and elimination phases for glucuronide/sulfate conjugates, respectively.

The integrated solutions for plasma concentrations of unchanged quercetin (in compartment 1) and its glucuronide/sulfate conjugates (in compartment 3) after an oral administration are:

$$C_1(t) = \frac{F_1 D K_{a1}}{V_1} \cdot \left[\frac{k_{21} - K_{a1}}{(\alpha_1 - K_{a1})(\beta_1 - K_{a1})} e^{-K_{a1} t} + \frac{K_{21} - \alpha_1}{(K_{a1} - \alpha_1)(\beta_1 - \alpha_1)} e^{-\alpha_1 t} + \frac{K_{21} - \beta_1}{(K_{a1} - \beta_1)(\alpha_1 - \beta_1)} e^{-\beta_1 t}\right] \quad \text{(A29)}$$

$$C_3(t) = \frac{F_1 D K_{a1} K_f}{V_3} \cdot [A_1 e^{-K_{a1} t} + A_2 e^{-\alpha_1 t} + A_3 e^{-\beta_1 t} + A_4 e^{-\alpha_2 t} + A_5 e^{-\beta_2 t}] + \frac{F_2 D K_{a2}}{V_3} \cdot \left[B_1 e^{-K_{a2} t} + B_2 e^{-\alpha_2 t} + B_3 e^{-\beta_2 t}\right] \quad \text{(A30)}$$

where

$$A_1 = \frac{(K_{21} - K_{a1})(K_{43} - K_{a1})}{(\alpha_1 - K_{a1})(\beta_1 - K_{a1})(\alpha_2 - K_{a1})(\beta_2 - K_{a1})} \quad \text{(A31)}$$

$$A_2 = \frac{(K_{21} - \alpha_1)(K_{43} - \alpha_1)}{(K_{a1} - \alpha_1)(\beta_1 - \alpha_1)(\alpha_2 - \alpha_1)(\beta_2 - \alpha_1)} \quad \text{(A32)}$$

$$A_3 = \frac{(K_{21} - \beta_1)(K_{43} - \beta_1)}{(K_{a1} - \beta_1)(\alpha_1 - \beta_1)(\alpha_2 - \beta_1)(\beta_2 - \beta_1)} \quad \text{(A33)}$$

$$A_4 = \frac{(K_{21} - \alpha_2)(K_{43} - \alpha_2)}{(K_{a1} - \alpha_2)(\alpha_1 - \alpha_2)(\beta_1 - \alpha_2)(\beta_2 - \alpha_2)} \quad \text{(A34)}$$

$$A_5 = \frac{(K_{21} - \beta_2)(K_{43} - \beta_2)}{(K_{a1} - \beta_2)(\alpha_1 - \beta_2)(\beta_1 - \beta_2)(\alpha_2 - \beta_2)} \quad \text{(A35)}$$

$$B_1 = \frac{K_{43} - K_{a2}}{(\alpha_2 - K_{a2})(\beta_2 - K_{a2})} \quad \text{(A36)}$$

$$B_2 = \frac{K_{43} - \alpha_2}{(K_{a2} - \alpha_2)(\beta_2 - \alpha_2)} \quad \text{(A37)}$$

$$B_3 = \frac{K_{43} - \beta_2}{(K_{a2} - \beta_2)(\alpha_2 - \beta_2)} \quad \text{(A38)}$$

REFERENCES

1. A. Crozier, M. E. J. Lean, M. S. McDonald, and C. Black. Quantitative analysis of the flavonoid content of commercial tomatoes, onions, lettuce, and celery. *J. Agric. Food Chem.* **45**:590–595 (1997).
2. L. Bravo. Polyphenols: chemistry, dietary sources, metabolism, and nutritional significance. *Nutr. Rev.* **56**:317–333 (1998).
3. W. Zheng and S. Y. Wang. Antioxidant activity and phenolic compounds in selected herbs. *J. Agric. Food Chem.* **49**: 5165–5470 (2001).
4. M. G. L. Hertog and P. C. H. Hollman. Potential health effects of the dietary flavonol quercetin. *Eur. J. Clin. Nutr.* **50**:63–71 (1996).
5. J. V. Formica and W. Regelson. Review of the biology of quercetin and related bioflavonoids. *Food Chem. Toxicol.* **33**: 1061–1080 (1995).
6. D. A. Shoskes, S. I. Zeitlin, A. Shahed, and J. Rajfer. Quercetin in men with category III chronic prostatitis: a preliminary prospective, double-blind, placebo-controlled trial. *Urology* **54**:960–963 (1999).
7. F. Katske, D. A. Shoskes, M. Sender, R. Poliakin, K. Gagliano, and J. Rajfer. Treatment of interstitial cystitis with a quercetin supplement. *Tech. Urol.* **7**:44–46 (2001).
8. E. U. Graefe, H. Derendorf, and M. Veit. Pharmacokinetics and bioavailability of the flavonol quercetin in humans. *Int. J. Clin. Pharmacol. Ther.* **37**:219–233 (1999).
9. P. Ader, A. Wessmann, and S. Wolffram. Bioavailability and metabolism of the flavonol quercetin in the pig. *Free Radic. Biol. Med.* **28**:1056–1067 (2000).
10. E. J. Oliveira, D. G. Watson, and M. H. Grant. Metabolism of quercetin and kaempferol by rat hepatocytes and the identification of flavonoid glycosides in human plasma. *Xenobiotica* **32**:279–287 (2002).
11. Y. Liu, Y. Liu, Y. Dai, L. Xun, and M. Hu. Enteric disposition and recycling of flavonoids and ginkgo flavonoids. *J. Altern. Complement. Med.* **9**:631–640 (2003).
12. J. A. Conquer, G. Maiani, E. Azzini, A. Raguzzini, and B. J. Holub. Supplementation with quercetin markedly increases

plasma quercetin concentration without effect on selected risk factors for heart disease in healthy subjects. *J. Nutr.* **128**:593–597 (1998).
13. J. Nishigaki, S. Suzuki, J. Yui, and A. Shigematsu. Distribution volume of three 99mTc-labeled compounds in the rat liver with time after intraportal and intravenous injections. *Biol. Pharm. Bull.* **18**:1705–1709 (1995).
14. J. Nishigaki, Y. Suzuki, and A. Shigematsu. A novel method for measuring the hepatic first-pass effect and metabolic rate of L-3,4-dihydroxyphenylalanine (DOPA), diazepam and inulin in rat liver. *Biol. Pharm. Bull.* **21**:735–740 (1998).
15. J. F. Marier, P. Vachon, A. Gritsas, J. Zhang, J. P. Moreau, and M. P. Ducharme. Metabolism and disposition of resveratrol in rats: extent of absorption, glucuronidation, and enterohepatic recirculation evidenced by a linked-rat model. *J. Pharmacol. Exp. Ther.* **302**:369–373 (2002).
16. S. Ueda, K. Yamaoka, and T. Nakagawa. Effect of pentobarbital anaesthesia on intestinal absorption and hepatic first-pass metabolism of oxacillin in rats, evaluated by portal-systemic concentration difference. *J. Pharm. Pharmacol.* **51**:585–589 (1999).
17. D. J. Hoffman, T. Seifert, A. Borre, and H. N. Nellans. Method to estimate the rate and extent of intestinal absorption in conscious rats using an absorption probe and portal blood sampling. *Pharm. Res.* **12**:889–894 (1995).
18. I. Erlund, G. Alfthan, H. Siren, K. Ariniemi, and A. Aro. Validated method for the quantitation of quercetin from human plasma using high-performance liquid chromatography with electrochemical detection. *J. Chromatogr. B Biomed. Sci. Appl.* **727**:179–189 (1999).
19. Y. C. Hou, P. D. Chao, H. J. Ho, C. C. Wen, and S. L. Hsiu. Profound difference in pharmacokinetics between morin and its isomer quercetin in rats. *J. Pharm. Pharmacol.* **55**:199–203 (2003).
20. L. B. Sheiner and S. L. Beal. Some suggestions for measuring predictive performance. *J. Pharmacokinet. Biopharm.* **9**:503–512 (1981).
21. C. Manach, O. Texier, C. Morand, V. Crespy, F. Regerat, C. Demigne, and C. Remesy. Comparison of the bioavailability of quercetin and catechin in rats. *Free Radic. Biol. Med.* **27**:1259–1266 (1999).
22. C. Manach, C. Morand, V. Crespy, C. Demigne, O. Texier, F. Regerat, and C. Remesy. Quercetin is recovered in human plasma as conjugated derivatives which retain antioxidant properties. *FEBS Lett.* **426**:331–336 (1998).
23. C. Morand, V. Crespy, C. Manach, C. Besson, C. Demigne, and C. Remesy. Plasma metabolites of quercetin and their antioxidant properties. *Am. J. Physiol.* **275**:R212–R219 (1998).
24. I. Ueno, N. Nakano, and I. Hirono. Metabolic fate of ^{14}C-quercetin in the ACI rat. *Jpn. J. Exp. Med.* **53**:41–50 (1983).
25. R. Gugler, M. Leschik, and H. J. Dengler. Disposition of quercetin in man after single oral and intravenous doses. *Eur. J. Clin. Pharmacol.* **9**:229–234 (1975).
26. D. R. Ferry, A. Smith, J. Malkhandi, D. W. Fyfe, P. G. de Takats, D. Anderson, J. Baker, and D. J. Kerr. Phase I clinical trial of the flavonoid quercetin: pharmacokinetics and evidence for *in vivo* tyrosine kinase inhibition. *Clin. Cancer Res.* **2**:659–668 (1996).
27. T. Walle, U. K. Walle, and P. V. Halushka. Carbon dioxide is the major metabolite of quercetin in humans. *J. Nutr.* **131**:2648–2652 (2001).
28. A. R. Rechner, G. Kuhnle, P. Bremner, G. P. Hubbard, K. P. Moore, and C. A. Rice-Evans. The metabolic fate of dietary polyphenols in humans. *Free Radic. Biol. Med.* **33**:220–235 (2002).
29. H. P. Noteborn, E. Jansen, S. Benito, and M. J. Mengelers. Oral absorption and metabolism of quercetin and sugar-conjugated derivatives in specific transport systems. *Cancer Lett.* **114**:175–177 (1997).
30. K. A. Khaled, Y. M. El-Sayed, and B. M. Al-Hadiya. Disposition of the flavonoid quercetin in rats after single intravenous and oral doses. *Drug Dev. Ind. Pharm.* **29**:397–403 (2003).
31. P. C. Hollman, J. M. van Trijp, M. J. Mengelers, J. H. de Vries, and M. B. Katan. Bioavailability of the dietary antioxidant flavonol quercetin in man. *Cancer Lett.* **114**:139–140 (1997).
32. J. M. Van Den Hof. Structural identifiability of linear compartmental system. *IEEE Trans. Automat. Contr.* **43**:800–818 (1998).